

# Theoretical Investigations on the Solvation Process

## II. The Monohydrated Associates of Some Three-Membered Ring Molecules

GIULIANO ALAGONA, RENZO CIMIRAGLIA, EOLO SCROCCO, and JACOPO TOMASI

Laboratorio di Chimica Quantistica ed Energetica Molecolare del C.N.R.,  
Via Risorgimento 35, I-51100 Pisa, Italy

Received December 23, 1971

The conformation energies for monohydrated associates  $M \cdot H_2O$ , where M stands for oxirane, aziridine, oxaziridine and cyclopropene, have been obtained by using an electrostatic method, tested in a preceding paper, which relies on SCF molecular potentials calculated exactly. Stable associates have been found in the heterogroup region as well as near the bent bonds (single or double).

A discussion is made on the errors in calculating thermodynamic properties for such associates in gas phase by using *a priori* calculations. As a numerical example the free energy change in the association process is compared for two monohydrated associates of aziridine.

Die Konformationsenergien für Anlagerungsverbindung  $M \cdot H_2O$ , wobei M für Oxiran, Aziridin, Oxaziridin und Cyclopropen steht, werden mit einer elektrostatischen Methode berechnet. Dieses Verfahren wurde in einer vorhergehenden Veröffentlichung getestet und beruht auf exakt berechneten SCF-Molekülpotentialen. Stabile Anlagerungsverbindungen wurden für Konformationen gefunden, bei denen das Wassermolekül in der Nähe der Heterogruppe oder der gezogenen Einfach- oder Doppelbindung liegt. Die Fehler bei der Berechnung thermodynamischer Eigenschaften für derartige Anlagerungsverbindungen in der Gasphase werden abgeschätzt. Als ein numerisches Beispiel wird die Differenz der freien Energie bei der Anlagerung für zwei Anlagerungsverbindungen von Aziridin und Molekül Wasser verglichen.

### 1. Introduction

In a preceding paper [1] (hereafter called I) we proposed and tested a simple procedure useful to obtain a qualitative prediction of the most stable conformations of molecular hydration associates. Such a procedure must be considered only as a guide to reducing the number of geometries to be examined with correct quantum-mechanical methods.

The simple case of a monohydration associate AB where A stands for water and B is a molecule having at least a polar (hydrophilic) group is studied here using the electrostatic approach of paper I. Once the distance between the water molecule and the group chosen for solvation is determined, it is assumed that the changes of the interaction energy with orientation are solely controlled by the shape of the electrostatic fields generated by the two molecules. According to this assumption (the "electrostatic assumption"), the interaction energy can be written as:

$$\Delta E = \int d\tau_1 \left[ q_A(x_1) - \sum_{\alpha} Z_{\alpha} \delta(x_1 - x_{\alpha}) \right] \cdot \int d\tau_2 \left[ q_B(x_2) - \sum_{\beta} Z_{\beta} \delta(x_2 - x_{\beta}) \right] \cdot \frac{1}{|x_1 - x_2|} \quad (1)$$

$\varrho_A(\mathbf{x}_1)$  and  $\varrho_B(\mathbf{x}_2)$  are the electronic density functions of the two single molecules,  $\sum_{\alpha}^{\text{nucl}} Z_{\alpha} \delta(\mathbf{x}_1 - \mathbf{x}_{\alpha})$  is the nuclear charge density distribution of A, etc. The second integral of the right-hand side of Eq. (1) represents the electrostatic potential produced by molecule B. One can therefore write:

$$\Delta E = \int d\tau_1 \left[ \varrho_A(\mathbf{x}_1) - \sum_{\alpha} Z_{\alpha} \delta(\mathbf{x}_1 - \mathbf{x}_{\alpha}) \right] V_B(\mathbf{x}_1). \quad (2)$$

A partial justification of this assumption may be drawn, *a posteriori*, by examining the partition of the hydrogen-bond energy of associates thus far performed on *ab initio* calculations. From such analysis on  $\text{H}_2\text{O}$  dimer [2], formamide dimer [3], and  $\text{H}_2\text{CO}-\text{H}_2\text{O}$  associate [4], it was actually found that the coulombic portion of the interaction energy (i.e. the electrostatic energy) is nearly equal to the SCF interaction energy for large separations, beginning from distances a little greater than the equilibrium one. This trend is due to a cancellation, in this distance range, of the exchange, polarization and charge transfer portion of the energy<sup>1</sup>. At the equilibrium distance the coulombic portion becomes greater than the SCF interaction energy: for the three associates here considered the differences are, respectively: 1.4 kcal/mole (22%), 1.2 kcal/mole (16%) and 1.2 kcal/mole (34%).

As regards the variation of the interaction energy with respect to the reciprocal orientation of the two partners, the available data on the three systems considered, show that the SCF interaction energy and its coulombic portion run in a noticeably parallel fashion [1-4]. A unique exception concerns a set of conformations of the  $\text{H}_2\text{CO}-\text{H}_2\text{O}$  associate (model B of Ref. [4]), where however the  $\text{O}\cdots\text{H}\cdots\text{O}$  distance undergoes remarkable changes during the rotation involved.

As a practical method to calculate the electrostatic interaction energy, in I it was proposed to use an approximation of Eq. (2), where the molecular potential  $V_B(\mathbf{x}_1)$  is rigorously obtained *via* SCF MOLCAO calculations and the water molecule charge distribution (molecule A in Eq. (2)) is replaced by a suitable point-charge set which has the same dipole and quadrupole moments as those of a SCF wavefunction. This point-charge distribution also adequately reproduces in the neighbouring regions the same electrostatic potential as is calculated from a SCF wavefunction of  $\text{H}_2\text{O}$ . The interaction energy is then reduced to the simple sum:

$$\Delta E = \sum_k q_k(\mathbf{k}) V_B(\mathbf{k}), \quad (3)$$

where  $q_k$  are the values of the point charges, which are placed at the points  $\mathbf{k}$ .

In paper I this procedure was checked, with fairly encouraging results, on the water dimer. In the present paper we will use Eq. (3) firstly to search for the most stable conformations of monohydration associates for some three-membered ring molecules, secondly to obtain a first guess about the most important contributions to the thermodynamic properties of such associates. The electrostatic potentials

<sup>1</sup> We have adopted here the terminology of Ref. [4] to which reference is made for detailed definitions. We note here that the electrostatic energy as defined by Kollman and Allen [5] in their analysis of  $\text{H}_2\text{O}$  and HF dimers is somewhat different.

$V_B$  of the cyclic molecules here considered are taken from previous SCF MOLCAO calculations [6, 7]; the point charge model for  $H_2O$  is the same as in paper I.

The electrostatic method does not allow one to find the equilibrium distances between the two associated molecules. Reasonable distances, selected with reference to the experimental one of other hydrogen-bond associates, were employed throughout our calculations, but, as a result of several checks with other distances, we can state that the main conclusions of the conformational analysis do not depend considerably on the value employed.

## 2. Choice of a Reference System for the Geometry of the Associates

The associates between three membered ring molecules and water, both species being considered as rigid bodies, possess six internal degrees of freedom, three for determining the position of a point in the  $H_2O$  molecule – which we always chose as the oxygen nucleus – and three for describing the orientation of water with respect to the organic molecule.

For the first three degrees of freedom we chose polar systems differing according to the hydration zone we are interested in. All polar systems employed have the polar axis lying on the ring plane, perpendicular to a bond and passing through the opposite nucleus (an arrow in the figures indicates the positive direction). When hydration of a heteroatom is considered, the origin of the reference system will be in the heteroatom nucleus whereas, when the hydration of a ring bond is considered, it will be in this very bond. In all cases the azimuthal  $\phi$  angles will be measured from the ring plane. Typical examples are shown in Figs. 1 and 11.

As regards the second three degrees of freedom, we shall describe them by three rotation angles about three orthogonal axes  $\xi$ ,  $\eta$  and  $\zeta$  defined as follows: the  $\eta$  axis connects the O nucleus of water to the polar system center, the  $\zeta$  axis is parallel to the ring plane and the  $\xi$  axis is determined by the left-handedness of the system.

Associates having the same values of the polar coordinates will be referred to as *conformations* belonging to the same *configuration*. Given a configuration, a starting conformation must be defined; this will be done in the text according to the particular cross-section of the energy hypersurface we are interested in. In such a way it is possible to define each set of conformations considered in this paper in terms of rotations around an axis alone. For the reader's convenience we have reported for each cross section (Figs. 1–12) a sketch of the starting conformation together with an indication of the direction of axes and of the rotation involved. Such a sketch will be also useful for a complete definition of the azimuthal  $\phi$  angles, allowance being made that we assume as origin the molecular half-plane on the left of the figure.

## 3. Monohydrates of Oxirane: $(CH_2)_2O \cdot H_2O$

Chemical intuition suggests that association of oxirane with a water molecule will occur through a hydrogen-bond where the  $H_2O$  molecule acts as a proton donor and the oxygen atom of oxirane as acceptor group. We actually find the

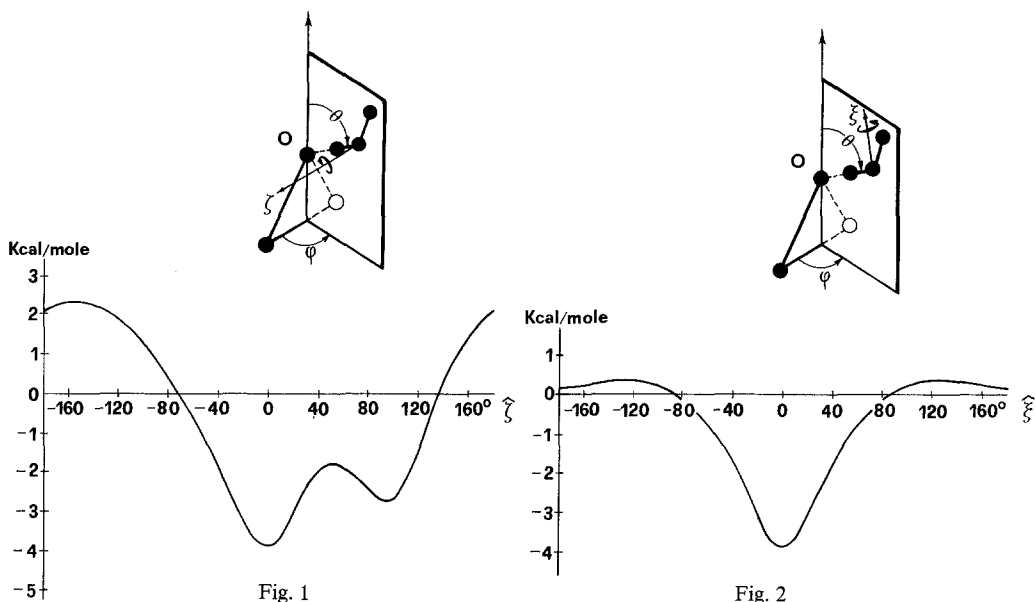


Fig. 1

Fig. 2

Fig. 1. Interaction energy between oxirane and water in the associate  $(\text{CH}_2)_2\text{O} \cdot \text{H}_2\text{O}$ . Rotation of the  $\text{H}_2\text{O}$  molecule around its  $\zeta$  axis. For the position of  $\text{H}_2\text{O}$  see the text

Fig. 2. Interaction energy in the associate  $(\text{CH}_2)_2\text{O} \cdot \text{H}_2\text{O}$ . Rotation of the  $\text{H}_2\text{O}$  molecule around its  $\xi$  axis

most stable associate ( $\Delta E = -3.8$  kcal/mole) at  $\phi = 90^\circ$  and  $\theta = 63^\circ$  (or in the equivalent position at  $\phi = 270^\circ$ ,  $\theta = 63^\circ$ ), i.e. with a direction of the O—O axis almost corresponding to that of an oxirane O lone pair<sup>2</sup>. Moreover, in the most stable conformation the O—H bond directly involved in the association is exactly collinear with the O—O axis. This can be verified by the aid of Figs. 1, 2, 3 where some cross-sections of the energy hypersurface, related to conformations pertaining to the most stable configuration, are reported.

Fig. 1 refers to conformations differing among them by a rotation about the  $\zeta$  axis. The starting conformation (sketched in the figure) is the most stable: the  $\text{H}_2\text{O}$  molecule lies in the plane perpendicular to the ring with a O—H bond pointing directly towards the heteroatom. The second minimum, relating to a rotation of  $\zeta = 96^\circ$ , again corresponds to an almost linear hydrogen bond. The non equivalence of the two minima and the slight deviation from linearity of the second stable conformation ( $\zeta = 96^\circ$  instead of  $104^\circ$ ) are presumably due to destabilizing electrostatic effects of the  $\text{CH}_2\text{—CH}_2$  group.

A rotation around  $\xi$  axis is decidedly hindered (see Fig. 2), the starting conformation being at the bottom of a fairly deep hole. On the contrary the rotation around  $\eta$  axis (Fig. 3) is almost free: the barrier height is 1.4 kcal/mole.

The picture of the association of water to the ring oxygen obtained with the present method corresponds to a classical linear hydrogen bond. It may be of

<sup>2</sup> The localization of the molecular orbitals of oxirane, performed in Ref. [6], leads to a couple of oxygen lone pair orbitals having its charge centers at  $\theta = 68^\circ$  ( $\phi = 90^\circ$  and  $270^\circ$ ).

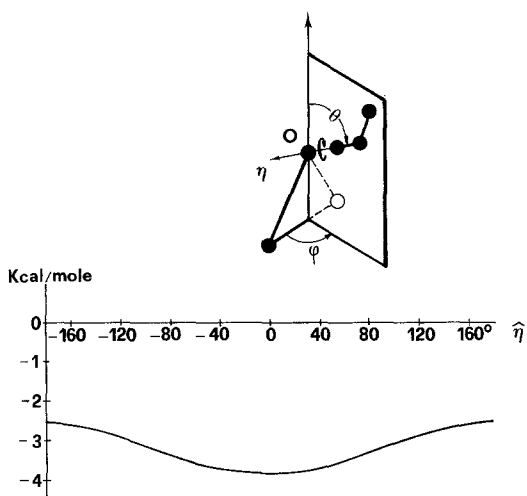


Fig. 3

Fig. 3. Interaction energy in the associate  $(\text{CH}_2)_2\text{O} \cdot \text{H}_2\text{O}$ . Rotation of the  $\text{H}_2\text{O}$  molecule around its  $\eta$  axis

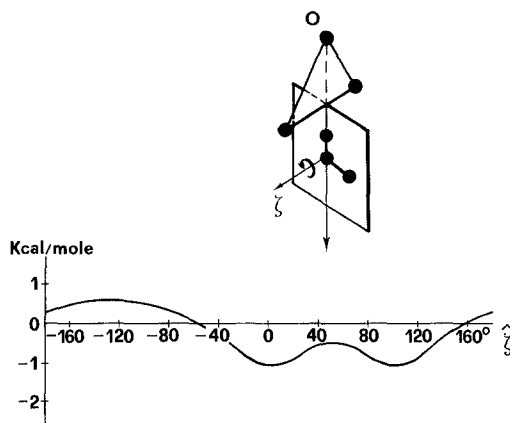


Fig. 4

Fig. 4. Interaction energy between  $(\text{CH}_2)_2\text{O}$  and  $\text{H}_2\text{O}$ . Hydrocarbon zone: rotation around  $\zeta$  axis

some interest to point out that the “bifurcated” associate, with the  $\text{H}_2\text{O}$  molecule perpendicular to the ring plane and with the two O—H bonds symmetrically pointing towards the two lone pairs, is not favoured.

For all the configurations thus far considered the  $r$  value was kept constant at  $r = 2.76 \text{ \AA}$ ; this value, as above said, was selected according to experimental values of other hydrogen bonds, but as a check we have repeated the calculations using larger and smaller values ( $\Delta r = \pm 0.2 \text{ \AA}$ ) and found that the position of the minima and the shape of energy hypersurface did not change significantly.

The electrostatic potential maps of oxirane (Figs. 10 and 11 of Ref. [6]) show that the direction of the hydrogen bonds does not correspond exactly either to the direction of the minima of  $V(x)$  ( $\theta \simeq 54^\circ$ ) or to the directions of larger potential gradient. It is convenient to point out here that we shall not search close relations between potential gradient and geometry of associates because it would correspond to reducing the  $\text{H}_2\text{O}$  charge distribution to a single point dipole. It is a well known fact that such an approximation is largely unsatisfactory for several reasons, the first being that it is not able to reproduce the directional properties of the hydrogen bond.

Keeping in mind such cautionary remarks, one can however use the shape and the sign of the electrostatic potential to obtain a first indication of the regions of the outer molecular space where association is more probable. For example, from Figs. 10 and 11 of Ref. [6] a second minimum of  $V(x)$  for oxirane in the region near the bent C—C bond is evident. The hydration of the C—C bond is indeed possible according to our model. The most stable configuration corresponds to  $\theta = 0^\circ$  in its polar system. The stabilization energy is decidedly lower than in the preceding case ( $-1.1 \text{ kcal/mole}$  against  $-3.8 \text{ kcal/mole}$ ). As an example the rotation around  $\zeta$  axis is shown in Fig. 4. The two minima correspond to two

symmetrical conformations, both having an O–H bond along the  $C_2$  symmetry axis of oxirane, while the  $H_2O$  molecule lies in the plane perpendicular to the ring. This is the best configuration we have found in this region. The electrostatic model does not evidence noticeable barriers for rotations around  $\eta$  axis; a single minimum appears for rotations around  $\xi$  axis (corresponding to the best conformation of Fig. 4). In this case, again, the shape of the conformation curves are not heavily dependent on the  $r$  value; the curve reported in Fig. 4 refers to an  $r$  value such as to allow a penetration of the van der Waals spheres of about 10%.

In this molecule each  $CH_2$  group is surrounded by a region of positive  $V(x)$  values (see again Fig. 10 in Ref. [6]) which could in principle lead to associates where the  $H_2O$  molecule acts as proton acceptor. In this zone we find so small a stabilization energy ( $\sim 0.2$  kcal/mole) as not to deserve here a more detailed analysis.

#### 4. Monohydrates of Aziridine: $(CH_2)_2NH \cdot H_2O$

When compared with oxirane, the situation for aziridine monohydrates is more complex. In the heterogroup region it will now be possible to have hydrogen bonds with the  $H_2O$  molecule acting both as proton acceptor (N–H bond region) and as donor (N lone pair region).

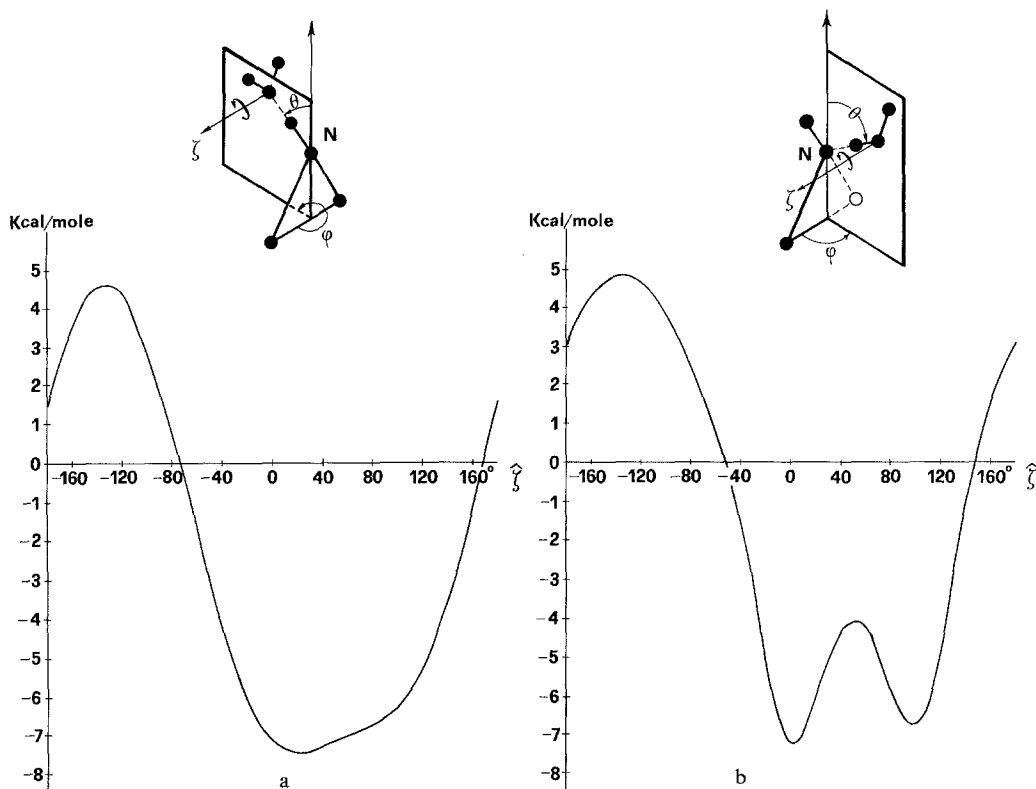


Fig. 5a and b. Interaction energy in the associate  $(CH_2)_2NH \cdot H_2O$ . Rotation of the  $H_2O$  molecule around its  $\zeta$  axis. a Association to the NH bond, b association to the N lone pair

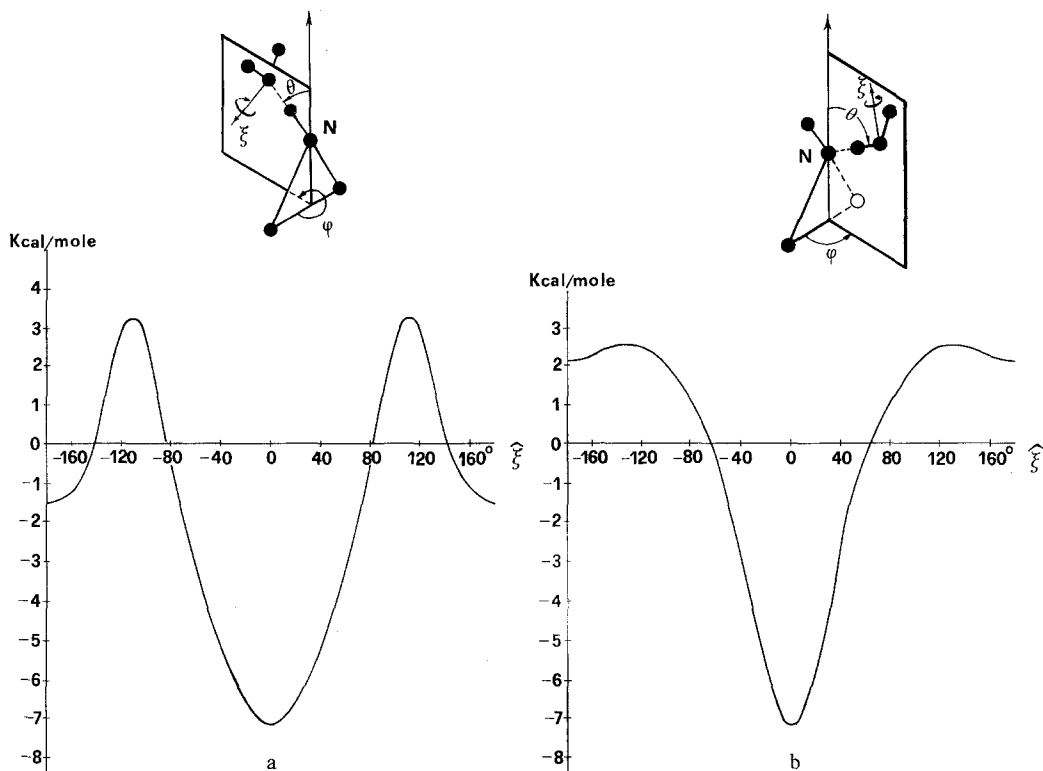


Fig. 6 a and b. As Fig. 5, rotations around  $\xi$  axes

We actually find in the N–H region a minimum of  $-7.3$  kcal/mole at  $\phi = 270^\circ$  and  $\theta = 68^\circ$  (the  $\text{H}_2\text{O}$  oxygen nucleus exactly lies in the line of the N–H bond), the most stable conformation having an oxygen lone pair almost collinear with the N–H bond. In the N lone pair region the minimum is found at  $\phi = 90^\circ$  and  $\theta = 62^\circ$ <sup>3</sup>; its value is nearly the same as in the preceding case ( $-7.1$  kcal/mole) but, as it will be shown immediately, the shape of the energy hypersurface is decidedly different.

In order to facilitate comparisons between the two associates, the conformation energy graphs are reported two by two in Figs. 5a, b; 6a, b; 7a, b. Figs. 5 refer to rotations around  $\zeta$  axis. Fig. 5a shows a trend of the stabilization energy very close to that found in the corresponding rotation of dimeric water (paper I, Fig. 6)<sup>4</sup>; we note that in the present case the starting conformation has the O lone pair center exactly collinear with the N–H bond. Fig. 5b is similar to the corresponding one of oxirane (Fig. 1 of this paper), although differences in depth and curvature are evident.

<sup>3</sup> The charge center of the N lone pair localized orbital lies at  $\theta = 56^\circ$ , while the minimum of  $V(\mathbf{x})$  is at  $\theta = 55^\circ$  (see Ref. [6]).

<sup>4</sup> The electrostatic model there employed was tailored on minimal basis set SCF wavefunctions: it is gratifying to observe that the far more accurate calculations of Hankins, Moskowitz and Stillinger on the  $\text{H}_2\text{O}$  dimer [8] confirm the shape of the curve in question.

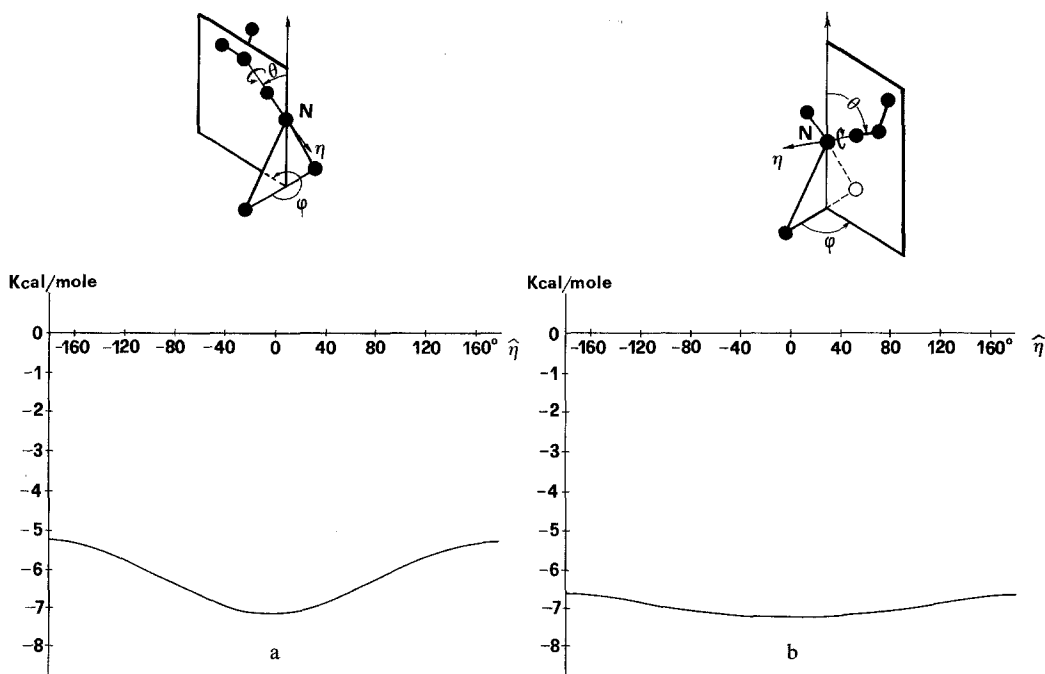


Fig. 7 a and b. As Fig. 5, rotations around  $\eta$  axes

Rotations about  $\zeta$  and  $\eta$  axes are reported in Figs. 6 and 7; in both cases the difference between the two associates are evident and will not be further discussed here. It is clear that such differences in the shape of the energy hypersurface between the two associates, if confirmed by more accurate calculations, could produce sensible differences in their thermodynamic stabilities. This topic will be considered later.

Solvation of the  $\text{CH}_2\text{-CH}_2$  group leads in aziridine to results very similar to those found in oxirane (Fig. 4). The minimum is slightly lower than in oxirane ( $\Delta E \approx -1.8$  kcal/mole) and corresponds to the same configuration. Oxirane had two equivalent conformations while in aziridine the most stable one has the  $\text{H}_2\text{O}$  molecule lying in the half plane which also contains the N lone pair.

### 5. Monohydrates of Oxaziridine: $\text{CH}_2\text{ONH} \cdot \text{H}_2\text{O}$

The main interest in studying the hypothetical water associates of  $\text{CH}_2\text{ONH}$  lies in the fact that oxaziridine contains at the same time in its ring the two heterogroups (O and NH) already seen separately.

The most stable configuration in the oxygen zone is found at  $\phi = 90^\circ$ ,  $\theta = 63^\circ$  ( $\Delta E = -3.7$  kcal/mole). A second minimum is found at  $\phi = 270^\circ$ ,  $\theta = 57^\circ$  ( $\Delta E = -3.5$  kcal/mole); this little difference in the minima is presumably due to the different electrostatic interaction with the NH bond and the N lone pair orbital. In this case, again, a correspondence between the most stable configuration and



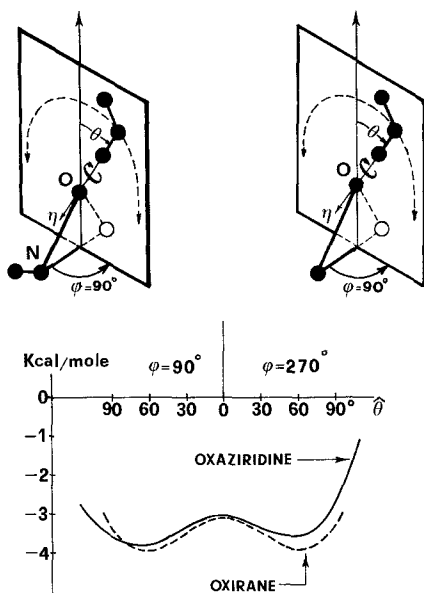


Fig. 8. Comparison of the stabilization energies in  $(\text{CH}_2)_2\text{O}$  and  $\text{CH}_2\text{ONH}$  monohydrates with association in the O ring region

the direction of lone pairs can be found: the localized lone pair orbitals of Ref. [7] have charge centers at  $\phi \simeq 90^\circ$ ,  $\theta \simeq 67^\circ$  and  $\phi \simeq 270^\circ$ ,  $\theta \simeq 67^\circ$  respectively.

Configuration curves are similar in oxirane and oxaziridine. In the first case the barrier height between the two equivalent configurations is about 0.9 kcal/mole while for oxaziridine associates we found that the higher of the two different barriers is about 0.7 kcal/mole. Fig. 8 reports for both molecules the stabilization energies for the best conformation of each configuration considered. In all cases the  $\xi$  and  $\zeta$  optimum angles are equal to zero, while the orientation of  $\text{H}_2\text{O}$  around the hydrogen bond changes with  $\theta$  angle and at the minimum corresponds to  $\hat{\eta} = 240^\circ$  for oxaziridine and to  $\hat{\eta} = 0^\circ$  for oxirane. The curves here reported refer to the best configurations we have found; however an analysis of the stabilization energy for configurations having the  $\text{H}_2\text{O}$  oxygen nucleus in planes different from that shown in Fig. 8 showed a relatively high freedom in the motion relating to the  $\phi$  coordinate.

Conformation curves for the oxaziridine associate in this oxygen zone are not reported; they are very similar to the corresponding one of oxirane (see Figs. 1-3).

The most stable configuration for the associate in the N-H region corresponds to  $\phi = 270^\circ$ ,  $\theta = 68^\circ$  (i.e. the same values as in the aziridine monohydrate), with a stabilization energy of  $-7.6$  kcal/mole. Fig. 9 shows the rotations around  $\zeta$  axis, starting from the conformation having the water O lone pair charge center on the N-H...O axis; the resemblance with Fig. 5a is very close. Also in this case the best conformation has not the lone pair charge center exactly collinear with the hydrogen bond axis: the angle between the N-H straight line and the oxygen lone pair center direction, which was about  $20^\circ$  in the aziridine case is now  $30^\circ$ .

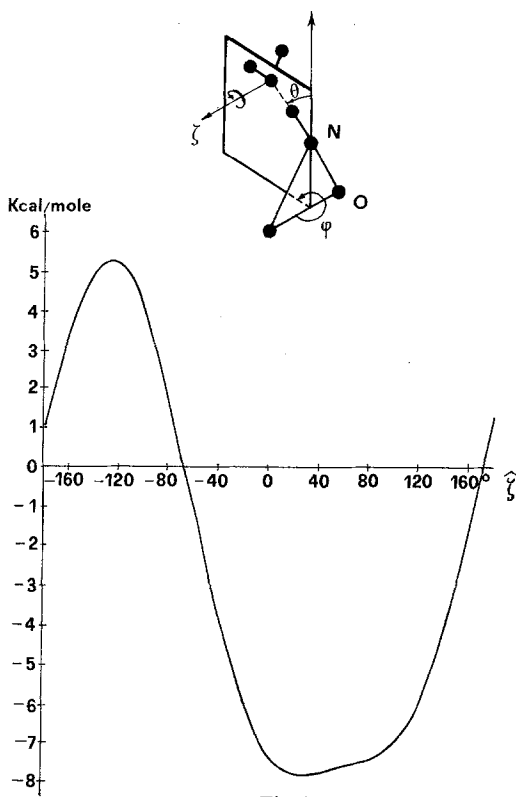


Fig. 9

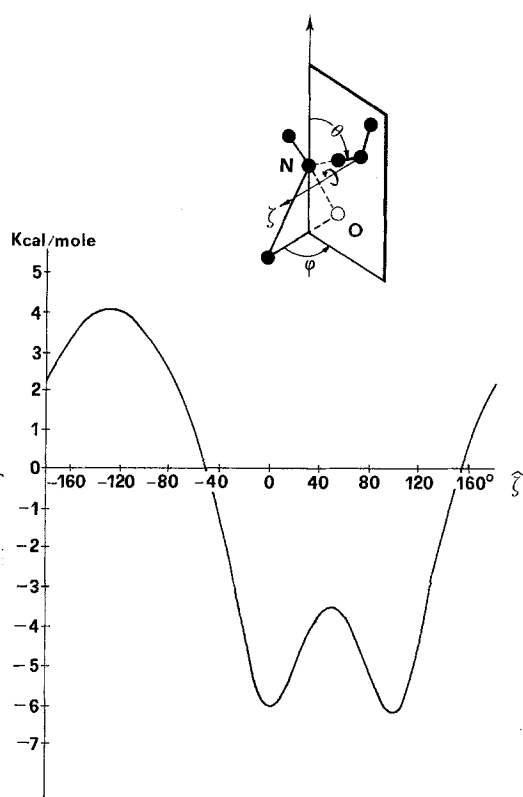


Fig. 10

Fig. 9. Interaction energy between  $\text{CH}_2\text{NHO}$  and  $\text{H}_2\text{O}$ . Association in the NH regionFig. 10. Interaction energy between  $\text{CH}_2\text{NHO}$  and  $\text{H}_2\text{O}$ . Association in the N lone pair region

Rotations around  $\eta$  axis (almost free) and around  $\zeta$  axis (a deep hole) are very similar to the corresponding ones of the aziridine monohydrate and are not reported here.

The association in the N lone pair region leads to a minimum at  $\phi = 90^\circ$ ,  $\theta = 63^\circ$  ( $\Delta E = -6.1$  kcal/mole). Such configuration is at the bottom of a relatively deep hole with respect to the  $\phi$  coordinate. Also in this case two conformations, nearly equivalent and both corresponding to linear  $\text{O}-\text{H}\cdots\text{N}$  bonds, are possible. Such conformations are evident in Fig. 10; a comparison with Fig. 5b shows that interactions with the oxygen atom of the ring lead to a small stabilization of the conformer having the second H atom pointing downwards. Other sections of the interaction energy hypersurface (rotations about  $\eta$  and  $\zeta$  axes) are again very similar to the corresponding one of aziridine and are not reported here.

From the comparison between oxaziridine and the two molecules of oxirane and aziridine, we could state, as a sort of conclusion, that both the geometry of most stable associate and the interaction energy do not change drastically when substitutions are made in a molecule. The changes we found can be explained in terms of electrostatic effects of the substituent groups.

## 6. Monohydrates of Cyclopropene: $(\text{CH})_2\text{CH}_2 \cdot \text{H}_2\text{O}$

For a study about the hydration of hydrocarbon groups we chose cyclopropene instead of the saturated analogue cyclopropane because the association near the C—C single bond has been already seen in oxirane and aziridine while the C=C double bond presents obvious interesting features<sup>5</sup>.

The electrostatic potential  $V(\mathbf{x})$  for cyclopropene has four nearly equivalent minima. The first two are in the region of the double bond and are symmetrically placed on either side of the ring plane (see Fig. 17 of Ref. [6]); the presence of such minima may be related to a description of a strained double bond system in terms of two banana bonds. The other two minima are near each C—C single bond, and are placed in the ring plane (see Fig. 18 of Ref. [6]).

We found four configurations of water monoassociate having practically the same energy. The first couple corresponds to the two double bond potential minima. In a polar reference frame centered on the midpoint of the C=C bond and with polar axis pointing outwards (see also Fig. 11) the best configurations are at  $\theta = 50^\circ$  (the minima of  $V(\mathbf{x})$  are at  $\theta = 58^\circ$  and the banana bond charge centers at  $\theta = 71^\circ$ ) and  $\phi = 90^\circ$  and  $270^\circ$ . The energy changes for variations of  $\theta$  are very small and the barrier height at  $\theta = 0^\circ$  is of the order of 0.5 kcal/mole. The best conformation ( $\Delta E = -2.9$  kcal/mole) has the  $\text{H}_2\text{O}$  molecule in the plane perpendicular to the ring, with a O—H bond pointing approximately towards the C=C midpoint while the other H nucleus is at a  $\theta$  angle greater than the O nucleus. A secondary minimum corresponds to a hydrogen bond made with the other O—H bond: see Fig. 11 where the starting conformation has the  $\text{H}\hat{\text{O}}\text{H}$  angle bisector pointing towards the polar axes center.

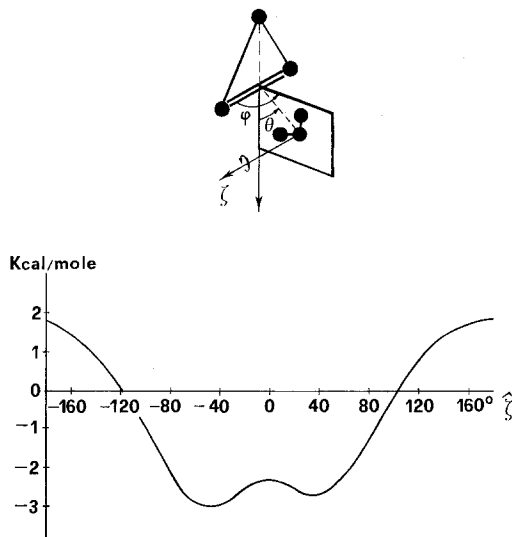


Fig. 11. Interaction energy between  $(\text{CH})_2\text{CH}_2$  and  $\text{H}_2\text{O}$ . Association in the C—C double bond region

<sup>5</sup> It is perhaps superfluous to remark that the trend of association of water to C—C and C=C bonds will surely change in going to unstrained molecules.

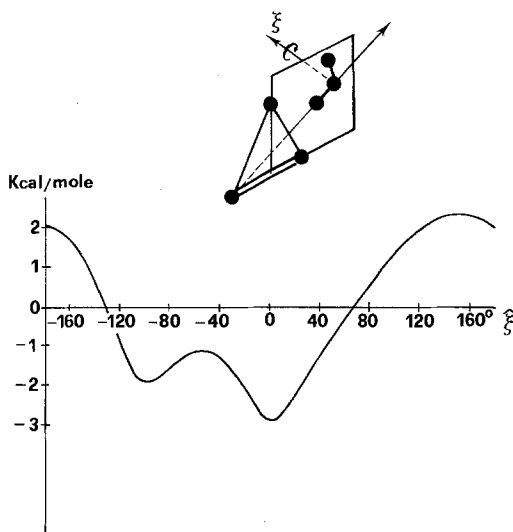


Fig. 12. As Fig. 11, association in the C—C single bond region

The second couple of symmetrical configurational minima is related to water association near the two C—C single bonds. One of such two configurations is depicted in Fig. 12 ( $\theta = 0^\circ$ ). In the best conformation ( $\Delta E = -2.9$  kcal/mole) the H<sub>2</sub>O molecule lies in the cyclopropene ring plane with an OH bond perpendicular to the C—C bond. The second OH bond, is directed as shown in the sketch of Fig. 12. Rotations around  $\xi$  axis show a second conformational minimum having the other OH almost perpendicular to the C—C bond.

Hydration of the CH<sub>2</sub> group leads to stabilization energies always less than 1 kcal/mole and no minima have been found; in this region the energy hypersurface presents a saddle point.

All results for cyclopropene have been checked by changing the distance of the water molecule from the relevant functional group (C=C and C—C) in the range 2.5–3.4 Å. Changes in the shape of the conformation (and configuration) curves are not observed, while, as expected, the absolute values of  $\Delta E$  show an  $r$  dependence analogous to that found in paper I for water dimer.

## 7. Thermodynamic Stability of the Associates

### a) Error Analysis with Use of SCF Energies

Thermodynamic information about the associates could be obtained through statistical methods once the potential energy hypersurface is known. In order to estimate the reliability of results, an analysis of the errors arising from the approximate knowledge of the energy hypersurface is demanded.

As an example, we will consider the problem of the thermodynamic stability of an associate, AB, in comparison either with the single species A and B, or with other associates.

The stability of the associate is directly related to the Gibbs free energy change in the association reaction



Assuming ideal gas behaviour and the molecules in their standard states, one gets:

$$\Delta F^\circ = F_{AB}^\circ - (F_A^\circ + F_B^\circ) = -D - RT \ln \frac{f^{AB} N}{f^A f^B}, \quad (5)$$

where  $N$  is Avogadro's number,  $D$  the dissociation energy of  $AB$  and the  $f$ 's are the molecular partition functions, *measured from the bottom* of the energy hypersurface.

The formation of the associate leads to six intermolecular vibration modes which have no counterparts in the separated molecules. These intermolecular degrees of freedom originate in 3 rotational and 3 translational modes of the individual molecules which disappear when association takes place and can be interpreted, in a first approximation, as a stretching mode ( $v_\sigma$ ), four bending ( $v_\delta$  and  $v_\gamma$ ) and one torsional ( $v_\tau$ ) mode. The other vibrational modes of the associate have analogs in motions already present in  $A$  or  $B$ . As a first approximation, one may assume the corresponding contribution to the partition function unchanged in going from separated molecules to the associate<sup>6</sup>.

Eq. (5) may be therefore simplified:

$$\Delta F^\circ = -D - RT \ln \left[ N \cdot \prod_{\alpha}^3 \frac{f_{tr\alpha}^{AB} f_{rot\alpha}^{AB}}{f_{tr\alpha}^A f_{rot\alpha}^A f_{tr\alpha}^B f_{rot\alpha}^B} \cdot \prod_{\beta}^6 f_{vib\beta}^{AB} \right]. \quad (6)$$

Where the three values of  $\alpha$  label the three inertia axes and the index  $\beta$  the six intermolecular vibration modes.

If calculated with *a priori* methods, practically all the terms of Eq. (6) are subject to errors:

a) Uncertainties in the geometry of the chemical species involved in reaction (4) are reflected in  $f_{rot}$  terms, through the corresponding inertia moments. If one assumes that the geometries of both  $A$  and  $B$  are known and that the association does not alter them appreciably, errors are essentially due to the uncertainty in the equilibrium distance between  $A$  and  $B$ . Assuming a comparatively large uncertainty range ( $\Delta r = \pm 0.2 \text{ \AA}$ ), for monohydration associates like those here considered the overall error in the rotational term  $\Delta RT \ln f_{rot}^{AB}$  amount to about 0.01 kcal/mole. Uncertainties in the reciprocal equilibrium orientation of  $A$  and  $B$  give rise to somewhat smaller errors.

<sup>6</sup> It is well known that the formation of a hydrogen bond considerably changes some vibration frequencies. In particular the stretching of the  $X-H$  bond may change of some hundreds of wave numbers. The contribution which such frequency shift gives to  $\Delta F^\circ$  can be evaluated as

$$\Delta [RT \ln f_\nu] = -\frac{1}{2} Nhc \cdot \Delta n - \Delta [RT \ln(1 - e^{-x})] \approx -\frac{1}{2} Nhc \cdot \Delta n$$

( $N$  being Avogadro's number,  $x = hcn/kT$  and  $\Delta n$  the shift in question measured in  $\text{cm}^{-1}$ ). The contribution is practically proportional to  $\Delta n$  because the frequency of the  $N-H$  stretching vibration is of the order of  $3000 \text{ cm}^{-1}$  and therefore the exponential term is completely negligible. Assuming for our weak hydrogen bonds a shift of  $50-250 \text{ cm}^{-1}$  one gets a contribution of  $\sim 0.07-0.36$  kcal/mole for  $\Delta F^\circ$ . This will be taken into account later.

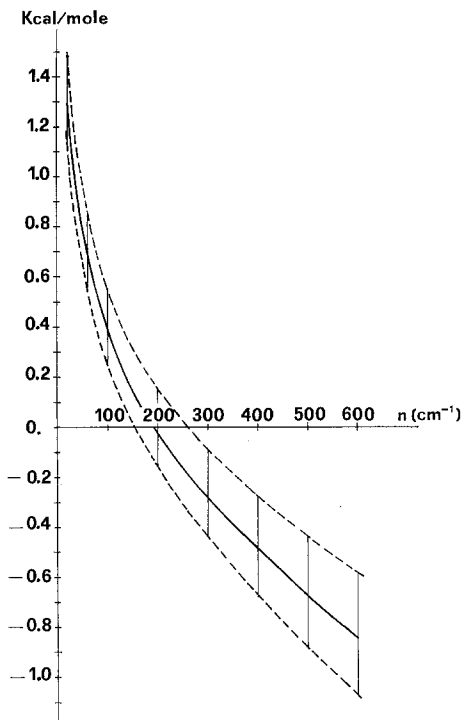


Fig. 13. Free energy contribution for a single harmonic vibration mode and its error bounds, assuming the error in the force constant to be 50%

b) More complicated is the analysis of the errors involved in the vibrational terms. Errors are due to uncertainties in quite a large portion of the potential energy hypersurface, which are propagated in a different manner according to the scheme adopted to evaluate frequencies (see, for example, Ref. [9]). Assuming here the harmonic approximation and a complete separation of the motions, the error may be reduced to be dependent, for each vibrational degree of freedom, on a single parameter, say the force constant  $k$  or the corresponding frequency  $\nu$ . It is easy to show that the error in the free energy change, due to a single vibrational mode, when energies are measured from the potential hypersurface minimum, is:

$$\Delta(RT \ln f_{\text{vib}_\beta}) \simeq -\frac{1}{2} Nhc \frac{1 + e^{-x_\beta}}{1 - e^{-x_\beta}} \Delta n. \quad (7)$$

With such error limits we find the situation depicted in Fig. 13: the free energy contribution due to a harmonic oscillator (full line) at a given calculated frequency  $n$  actually lies between the two dashed curves. For each vibrational degree the average error amounts to about  $\pm 0.2$  kcal/mole. If one assumes the error to be the same also for roto-vibrational modes the errors of all the intermolecular degrees of freedom and of the additional intramolecular X-H frequency changes produce an uncertainty conspicuous if compared with the expected  $\Delta F^\circ$  values (about  $\pm 1$  kcal/mole).

c) The last, but not least, source of error originates in the dissociation energy ( $D$ ) of the associate. Such a value may be expected to be sufficiently accurate only when using very good SCF calculations.

As an overall impression, approximate thermodynamic previsions on the stability of associates seem to be a very delicate problem. However when one is concerned in the *relative* stability of different associates, a rather large compensation among errors may be expected and therefore the hope of getting reliable results is not quite unrealistic.

### b) Error Analysis with Use of the Electrostatic Approximation

If we now pass on to analyze the electrostatic picture, it is evident that the method employed in this paper is too crude to give directly a prevision of sufficient precision for the free energy of formation. It may be however regarded as a guide to more rigorous calculations and may give a first guess to the *relative* stability of different associates.

From paper I the electrostatic method turns out to be able to give a description of the geometry of the associate sufficient for the rotational contribution, if the distances for hydrogen bonds are fixed according to experimental data. For the vibrational terms the error bounds assumed in the preceding section seem to be sufficient to include also the additional errors arising from the electrostatic approximation. As an example, in Table 1, a comparison is made among quadratic force constants for  $H_2O$  dimer as calculated with the electrostatic method and with two different MOLCAO SCF minimal basis set wavefunctions. As a further check we may quote a comparison with the accurate wavefunctions of Hankins, Moskowitz and Stillinger [8]. For the two sets of conformations reported in this paper (curve *A* and *B*, the reader is referred to the quoted paper for the identification of the curves) we have calculated the free energy contribution (by means of a numerical integration in the WKB approximation) and found:  $RT \ln f = 0.09$  kcal/mole for curve *A* and 0.32 kcal/mole for curve *B*. The same sections of the energy hypersurface, as calculated with the electrostatic model give, in the order, 0.04 and 0.26 kcal/mole<sup>7</sup>.

Table 1. Comparison of quadratic force constants for intermolecular vibrations in  $(H_2O)_2$ <sup>a</sup>

Force constant	Ref. [5] SCF	Ref. [1] SCF	Ref. [1] Electrostatic
$\partial^2 \epsilon / \partial \theta_1^2$	0.040986	0.0344	0.0274
$\partial^2 \epsilon / \partial \chi_1^2$	0.029775	0.0345	0.0344
$\partial^2 \epsilon / \partial \theta_2^2$	0.011711	0.0066	0.0050
$\partial^2 \epsilon / \partial \chi_2^2$	0.016972	—	0.0164
$\partial^2 \epsilon / \partial \phi^2$	0.001444	—	0.0006
$\partial^2 \epsilon / \partial R^2$	0.022877	0.0269	—

<sup>a</sup> The notation is the same as in Ref. [5]. All values in a.u.

<sup>7</sup> Both our electrostatic curve and curve *B* of Ref. [8] have quite a similar shape and the small differences between the partition functions are mainly due to our extrapolation of the higher portions of curve *B* of Ref. [8].

Table 2. Contributions to  $\Delta F^0$  for two different associates of aziridine<sup>a</sup>

Type of motion	Associate I $-RT\ln f$	Associate II
$\gamma(\xi)$	- 0.0002	+ 0.1073
$\gamma(\eta)$	+ 0.2221	+ 0.7979
$\tau(\zeta)$	- 0.5339	- 0.5234
$\delta(\xi)$	- 1.5256	- 1.3016
$\delta(\eta)$	- 1.5515	- 1.1758
$\sigma(\zeta)$	+ 0.0755	+ 0.0755
$-\sum_{\beta}^6 RT\ln f_{\text{vib}\beta}^{\text{AB}}$	- 3.31	- 2.02
$-\sum_{\alpha}^3 RT\ln \frac{f_{\text{rot}\alpha}^{\text{AB}}}{f_{\text{rot}\alpha}^{\text{A}} f_{\text{rot}\alpha}^{\text{B}}}$	1.55	1.53
$-\sum_{\alpha}^3 RT\ln \frac{f_{\text{tr}\alpha}^{\text{AB}}}{f_{\text{tr}\alpha}^{\text{A}} f_{\text{tr}\alpha}^{\text{B}}}$	41.65	41.65
$RT\ln N$	32.64	32.64
$-D$	- 7.3	- 7.1
$\Delta F^0$	- 0.05	1.42

<sup>a</sup> Expressed in kcal/mole.

In order to give a rough idea of the thermodynamic stability of the monohydrates considered in this paper, we have selected the two most stable associates of aziridine, the first (associate I) having the  $\text{H}_2\text{O}$  molecule attached to the N-H bond and the second (associate II) bound through the N lone pair. Assuming that in both cases during the association process the two molecules approach each other along the N-H-O axis direction (i.e. along the electrostatically most favoured channel) with the  $\text{H}_2\text{O}$  molecule disposed according to the most stable conformation, it is easy to visualize how six external modes of the separated molecules transform into six intermolecular vibrations.

The potential curves for associate I corresponding to  $\gamma(\xi)$ ,  $\gamma(\eta)$  and  $\tau(\zeta)$  motions have been already reported (Figs. 4a, 5a and 6a); curves for  $\delta(\xi)$  and  $\delta(\eta)$  are not reported for brevity; the curve corresponding to the stretching vibration [ $\sigma(\zeta)$ ] is not obtainable from the electrostatic model and the corresponding contribution to  $\Delta F^0$  was evaluated from a Morse function obtained from the stretching SCF curve of  $(\text{H}_2\text{O})_2$  with the  $D$  parameter taken from the present calculations. The corresponding contributions to  $\Delta F^0$  are reported in Table 2: they are calculated, according to the case, either in the harmonic approximation, or as rotators (restricted or free) or numerically in the WKB approximation.

The same procedure was utilized for associate II and the results are again reported in Table 2. At the bottom of this Table one can find also the other terms necessary to calculate  $\Delta F^0$  according to Eq. (6), the rotational contribution for the associates being related to the most stable geometries for I and II found in Sect. 4, and the dissociation energies being the corresponding stabilization energies reported in the same section.



According to the electrostatic model the most stable associate has the H<sub>2</sub>O molecule bound through the N–H bond (associate I). The equilibrium constants for the two associates are  $K_I = 1.093$  and  $K_{II} = 0.092$ . Such values do not seem completely outside any chemical plausibility, but it is necessary to repeat here that we have been mainly concerned in their relative – rather than absolute – values.

### References

1. Bonaccorsi, R., Petrongolo, C., Scrocco, E., Tomasi, J.: *Theoret. chim. Acta (Berl.)* **20**, 331 (1971).
2. Petrongolo, C., Scrocco, E., Tomasi, J.: Unpublished results.
3. Dreyfus, M., Pullman, A.: *Theoret. chim. Acta (Berl.)* **19**, 20 (1970).
4. Morokuma, K.: *J. chem. Physics* **55**, 1236 (1971).
5. Kollman, P. A., Allen, L. C.: *Theoret. chim. Acta (Berl.)* **18**, 399 (1970).
6. Bonaccorsi, R., Scrocco, E., Tomasi, J.: *J. chem. Physics* **52**, 5270 (1970).
7. — — — *Theoret. chim. Acta (Berl.)* **21**, 17 (1971).
8. Hankins, D., Moskowitz, J. W., Stillinger, F. H.: *J. chem. Physics* **53**, 4544 (1970).
9. Gerratt, J., Mills, I. M.: *J. chem. Physics* **49**, 1719 (1968).
10. Del Bene, J., Pople, J. A.: *J. chem. Physics* **52**, 4858 (1970).

Prof. Dr. J. Tomasi  
Laboratorio di Chimica  
Quantistica ed Energetica  
Molecolare del C.N.R.  
Via Risorgimento 35  
I-56100 Pisa, Italy